Vol. 5 No. 1 (2026)

Pakistan Journal of Medical & Cardiological Review

https://pakjmcr.com/index.php/1/about

Online ISSN 3007-2387

Print ISSN 3007-2379

# Integrated *In Vitro* and *In Silico* Evaluation of the Antibacterial Potential of Black Pepper (*Piper nigrum*) Against Multidrug-Resistant Pathogens

**Abdi Brahim** (Corresponding Author)
University of Agriculture Peshawar Email: abdib8653@gmail.com
**Hajra Fatima**
Department of microbiology, University of Karachi
Email: hajrafatima501@gmail.com
**Muhammad Irfan**
Institute of Chemical Engineering, Ural Federal University, Russia
Email: drkkhan374@gmail.com
**Aasma Akram**
Department Of Pharmaceutics, Faculty Of Pharmaceutical Sciences, Government College University Faisalabad Email: aasmaakram394@yahoo.com
**Sohaib Usman**
Department of bioscience, Comsats University Islamabad Sahiwal campus
Email: s.usman8@outlook.com
**Lawang Gurganari**
Provisional Institute Of Teacher Education Email: Lawang.uob86@gmail.com
**Sajida Parveen LMO**
Shakh Zaid hospital Quetta Email: Sajadamari@gmail.com

**Author Details**

**Keywords:** Antimicrobial Resistance, Black Pepper, In Vitro Study, In Silico Analysis, Bioactive Compounds.

**Received on 18 Feb 2026**
**Accepted on 18 Mar 2026**
**Published on 28 Mar 2026**

**Corresponding E-mail & Author*:**

**Abdi Brahim**
University of Agriculture Peshawar Email: abdib8653@gmail.com

**Abstract**

Antimicrobial resistance (AMR) is a global threat, leading to the failure of conventional antibiotics against multidrug-resistant (MDR) bacteria like Staphylococcus aureus and Escherichia coli, which cause severe infections. The growing resistance necessitates alternative antimicrobial agents. Black pepper (Piper nigrum), a common spice with medicinal properties, contains bioactive compounds such as piperine, flavonoids, and alkaloids that exhibit antimicrobial effects. However, scientific validation against resistant bacterial strains remains limited. This study evaluates black pepper's antibacterial effects against antibiotic-resistant bacteria using in vitro assays and in silico methods to analyze bioactive compound interactions with bacterial proteins. It is hypothesized that black pepper significantly inhibits bacterial growth by interfering with cell functions, supported by molecular docking and ADMET analysis. In vitro antibacterial assays, including agar well diffusion and minimum inhibitory concentration (MIC) tests, assess the efficacy of black pepper extracts, while in silico analysis predicts compound binding affinity, pharmacokinetics, and toxicity. Preliminary results indicate that black pepper exhibits moderate to strong antibacterial activity, with MIC values varying based on concentration and extraction method. In silico studies show strong binding affinities of bioactive compounds like piperine with bacterial proteins involved in resistance

mechanisms. ADMET analysis confirms favorable pharmacokinetic properties, suggesting potential for therapeutic use. These findings support black pepper as a promising natural antimicrobial agent, aligning in vitro and in silico results. Further research, including clinical studies and advanced formulations, is needed to enhance its efficacy and explore its role in combating AMR.

## Introduction

Antimicrobial resistance (AMR) has emerged as a significant global health threat, rendering many conventional antibiotics ineffective against bacterial infections ( Rajia et al., 2025). The overuse and misuse of antibiotics have accelerated the evolution of resistant bacterial strains, posing severe challenges to public health and clinical treatments ((LONGE et al., 2025). Among the most concerning antibiotic-resistant pathogens are *Staphylococcus aureus* and *Escherichia coli*, both of which are responsible for various infections ranging from minor skin infections to life-threatening conditions such as sepsis and pneumonia ( Dongre et al., 2025). The alarming rise of multidrug-resistant (MDR) bacteria necessitates the exploration of alternative therapeutic agents, particularly from natural sources, to combat microbial resistance effectively ( Kiranmayee et al., 2023).

Black pepper (*Piper nigrum*) a widely used spice in traditional medicine, has garnered attention for its potent bioactive compounds with antimicrobial properties( Yasir et al.,2024). It is rich in phytochemicals such as piperine flavonoids alkaloids and essential oils which have demonstrated antimicrobial activity against various bacterial strains including drug-resistant pathogens *( Raikwar et al ., 2025).* Studies suggest that black pepper exhibits antibacterial effects by disrupting bacterial cell membranes inhibiting biofilm formation and interfering with bacterial metabolic pathways *( Periferakis et al., 2025).* Given its natural origin and broad-spectrum activity black pepper holds promise as an alternative or adjunct antimicrobial agent to mitigate the AMR crisis *( Aydemir et al., 2024).*

To further explore the antibacterial potential of black pepper in silico approaches such as molecular docking ADMET (Absorption, Distribution, Metabolism, Excretion, and Toxicity) analysis and disease network studies provide valuable insights into its efficacy and safety *( Fratianni et al., 2026).* Molecular docking studies help predict the binding interactions of black pepper-derived compounds with bacterial target proteins aiding in the identification of potential antimicrobial agents *(Singh et al., 2024).* ADMET analysis ensures the pharmacokinetic and toxicity profiles of these compounds essential for drug development *(Daoud et al., 2021).* Additionally disease network analysis enables the understanding of complex interactions between bioactive molecules and bacterial resistance mechanisms *(Al-Azzawi et al., 2024).* Integrating in vitro antibacterial studies with computational approaches enhances the reliability of findings and accelerates the drug discovery process *( Iskandar, 2025).*

This study aims to evaluate the antibacterial effects of black pepper against resistant bacterial strains particularly *S. Aureus* and *E. coli* through in vitro experiments and in silico analyses *(Dongre et al., 2022)* . By combining traditional microbiological assessments with computational modeling, this research seeks to establish black pepper as a potential natural alternative in the fight against AMR contributing to the development of novel antimicrobial strategies *(* Rajia *et al., 2025*).

## Material and Method

### Preparation of Black Pepper leaf powder;

Fist we select Fresh black pepper leaves are carefully from mature plants avoiding any that are damaged diseased or insect-infested. The leaves are thoroughly rinsed under running water to remove dirt and contaminants then soaked in distilled water for a few minutes to eliminate residual pesticides before being patted dry with a clean

cloth or paper towels. For drying the leaves can be shade-dried for 5-7 days with proper air circulation to preserve bioactive compounds or if a quicker process is needed oven-dried at 40–50°C for 4–6 hours until completely dried. Once dried they are ground into a fine powder using a mixer blender or mechanical grinder and sieved if necessary for uniform particle size. The powdered black pepper leaves are then stored in an airtight container in a cool dry place away from moisture and direct sunlight ensuring freshness and potency for several months. This powder is used in herbal formulations and traditional medicine incorporated into animal feed for its antimicrobial properties and studied for pharmacological potential through in vitro and in silico analysis.

**Sample Collection and Preparation**

Tissue samples (heart, spleen, and lungs) collected from layer chickens (GPF Quetta) and homogenized in sterile phosphate-buffered saline (PBS) The homogenates were serially diluted to obtain microbial suspensions for culturing.

**Methanol extraction**

The ratio 70:.30 of methanol and distal water to Black pepper leaf powder was used to carry out the extraction. 25 mL of methanol and distal water solution was added to 7.5g of Black pepper leaf powder. The bottle was stirred firstly by hands carefully then with a magnetic stirrer for 24 hours at room temperature to extract the bioactive compounds. After 24 hours filter paper then & used 2 time with porcelain filter to filter the mixture in order to capture the liquid extract and the remaining plant materials were left behind in the samples bottle. The liquid was concentrated on sun light to remove the methanol and distal water for resulting extract was a concentrated extract methanol and distal water.

**Evaluation of Antimicrobial Activity Using MarConkey Agar and Nutrient-Rich Media**

The antimicrobial activity of the Black Pepper methanol & distal water extract and leaf powder was evaluated against microbes isolated from the heart, spleen and lungs of layer chickens and layer chicks. The inoculation procedure for evaluating antimicrobial activity using MacConkey agar and nutrient-rich media involves preparing bacterial suspensions from pure cultures by adjusting them to a standard turbidity, typically 0.5 McFarland. Using a sterile cotton swab, the bacterial suspension is evenly spread across the surface of MacConkey agar to differentiate lactose-fermenting from non-lactose-fermenting bacteria and on nutrient-rich media to support general bacterial growth. After allowing the plates to dry for a few minutes, antimicrobial agents or test compounds, such as black pepper extracts, are applied to designated wells or discs. The inoculated plates are then incubated at an optimal temperature, usually 37°C, for 18–24 hours. Post-incubation, bacterial growth is observed, and the zones of inhibition around the antimicrobial agents are measured to assess antibacterial efficacy. Detail procedure for preparation of Maccokney Agar and Nutrient rich media is provided in the supplementary section.

**Antimicrobial Activity Testing:**

Disc diffusion method sterile filter paper discs were impregnated with the methanol extract at different concentrations and placed onto the inoculated agar plates. The plates were incubated at 37°C for 24-48 hours and the zones of inhibition around the discs were measured to assess antimicrobial activity The plates were incubated and the zones of inhibition were measured. Direct application of Black Pepper leaf powder was Added onto the agar plates with 3 discs and 1 sample extract in it and the plates were incubated to observe any inhibition of microbial growth and minimum range to avoid any contamination.

**Black pepper Compounds evaluation from data bases**

We first created a dataset of 510 chemicals using the IMPPAT (Indian Medicinal Plants Photochemistry & Therapeutics) database. Next, we retrieved pertinent data such as drug-likeness ratings molecular weight & SMILES notation. Using Excel, we performed a number of filters to find compounds that showed promise. In order to select only compounds with a molecular weight more than 180 g/mol we first used a molecular weight filter yielding 254 compounds. 159 compounds were obtained after we used a bioavailability filter to choose compounds with a bioavailability score higher than 0.55. After applying a drug-likeness filter we were able to identify 15 compounds with a drug-likeness score higher than 0.72. We chose the top six compounds from this subset for additional examination.

***Insilico* ADMET analysis of Phyto-constituents of black pepper by pkCSM**

The ADMET characteristics investigation of chemicals we use a database pkCSM. We select the Small-molecule pharmacokinetics prediction tab after searching the pkCSM website. A new page appeared after selecting pkCSM computation & we entered the compound's smiles in the search tab. Next, we select the ADMET tab and proceed to the step two prediction model. We gathered the pharmacokinetic characteristics of every molecule from that page as soon as the new window appeared.

**Use of Protox 11 and Stoptox database for toxicity prediction of selected phytochemicals of black pepper**

We use the Protox 11 and Stoptox databases to study the toxicity characteristics of compounds. In Protox 11 we first search for the desired compounds navigate to the tox-prediction page enter the compounds SMILES in the search tab & make the necessary selections. We then proceed next by clicking Start Tox-Prediction after which a new window opens allowing us to collect the pro and pre values for each compound. Similarly, for toxicity analysis using the Stoptox database we first locate the Stoptox website link & navigate to its homepage. Once the website opens we click on the Stoptox home link leading to a new page where we enter the compound's smiles in the search tab. We then proceed to the second stage Anticipate Stoptox which opens a new window from which we extract the Stoptox value for each component.

**Comparable physiochemical properties of active compounds of black pepper using Way 2 drugs database and SwissADME database**

We used the **Way2Drug** database to analyze the probability of active compounds. First we make a log in account from way2drug website. After login to web page we go the predict new compound bar, then goes to smile tab and enter the respective smiles of compounds. And then we go for search, Antimycobacterial, Antibacteria, Bacterial efflux pump inhibitor, Lysozyme inhibitor, Phospholipase A2 inhibitor, Peptidoglycan glycosyltransferase inhibitor, RNA-directed RNA polymerase inhibitor, Lactoferrin, Defensin, Cathelicidin, Azurocidin, Bpi, Magainin, Cecropin, Protegrin, Histatin, Lactoferricin, Granulysin, Dermcidin, LL-37, Psoriasin, Calprotectin. The values of Pi and Pas were calculated from the website and put in the result table.

**Results**

**Active compounds**

Several active compounds, including 3,4-Methylenedioxycinnamic Acid, Benzyl benzoate, Kakuol, Elemol, Cubebol, & Moupinamide were selected on the basis of their molecular weight, bioavailability & drug-likeness. Furthermore, these substances were taken due to of their best bioactive qualities. Such as, bioavailability value of 0.85, 3,4-Methylenedioxycinnamic acid was the most bioavailable of these chemicals followed by Kakuol with a score of 0.73. Moupinamide, Cubebol, Elemol & benzoyl

benzoate all exhibited bioavailability scores of 0.55. The results for these substances were quite similar in terms of drug-likeness. Elemol, Cubebol, & Moupinamide all received drug-likeness scores of 0.72 but 3,4-Methylenedioxycinnamic Acid, Kakuol, and Benzyl Benzoate each had scores of 0.73. With a molecular weight of 192.17 g/mol 3,4-Methylenedioxycinnamic acid was the lowest, followed by Kakuol (194.19 g/mol). Elemol & Cubebol both had a molecular weight of 222.37 g/mol whereas benzoyl benzoate had a molecular weight of 212.25 g/mol. At 313.35 g/mol, moupinamide had the largest molecular weight (Table 1).

Table 1. Active chemical compound of black pepper and their structure, bioavailability, drug likeness and molecular weight.

| Compounds | Structures | Bioavailability | Drugs likeness | Molecular weight (g-mol) |
|---|---|---|---|---|
| 3,4-Methylenedioxycinnamic acid | 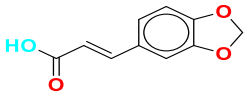 | 0.85 | 0.72 | 192.17 |
| Kakuol | 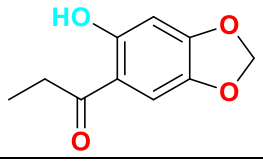 | 0.73 | 0.73 | 194.19 |
| Benzyl benzoate | 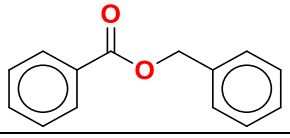 | 0.55 | 0.73 | 212.25 |
| Elemol | 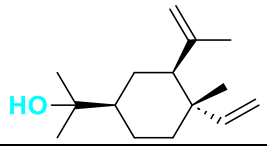 | 0.55 | 0.72 | 222.37 |
| Cubebol | 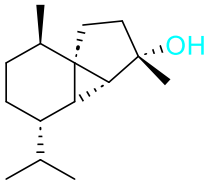 | 0.55 | 0.72 | 222.37 |
| Moupinamide | 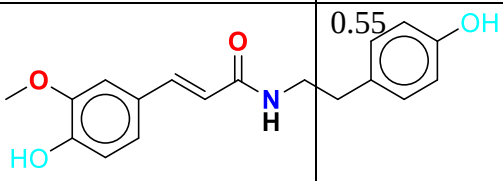 | 0.55 | 0.72 | 313.35 |

**Physicochemical and Pharmacokinetic Properties of active compounds of black pepper**

The six active compounds of black pepper exhibit diverse physicochemical properties influencing their permeability, solubility, and blood-brain barrier (BBB) penetration. Molecular weight varies from 192.04 g/mol (3,4-Methylenedioxycinnamic acid) to 313.13 g/mol (Moupinamide), impacting absorption and bioavailability. Hydrogen bond acceptors (HBA) and donors (HBD) affect solubility and membrane permeability, with Moupinamide having the highest hydrogen bonding potential, making it the most hydrophilic, while Elemol and Cubebol, with the lowest, are more lipophilic. MolLogP values indicate lipophilicity, with Elemol (4.62) being the most lipophilic and 3,4-Methylenedioxycinnamic acid (2.34) the least. MolLogS suggests that 3,4-Methylenedioxycinnamic acid and Moupinamide have better water solubility, whereas Benzyl benzoate and Elemol have the lowest. Polar surface area (PSA) affects passive permeability, with Benzyl benzoate (21.10 $A^2$) supporting high BBB

permeability, while Moupinamide (66.08 $A^2$) may have limited permeability. Molecular volume influences diffusion, with 3,4-Methylenedioxycinnamic acid having the smallest volume (191.44 $A^3$), aiding receptor interactions, while Moupinamide's larger volume (323.94 $A^3$) may hinder diffusion. Ionization states inferred from pKa suggest that Benzyl benzoate (24.45) remains neutral at physiological pH, enhancing permeability, whereas 3,4-Methylenedioxycinnamic acid (4.54) is more ionized, increasing solubility but reducing permeability. BBB scores indicate Benzyl benzoate (5.16) has the highest brain penetration potential, followed by Elemol and Cubebol (4.39), while Moupinamide (3.05) has the lowest due to its size and hydrogen bonding characteristics, limiting its ability to cross the BBB (Table 2).

**Table 2. Active chemical compound of black pepper, Physicochemical and Pharmacokinetic Properties by using mole soft database.**

| Compounds | Molecular formula | Number of HBA | Number of HBD | Mol LogP | Mol LogS | Mol PSA | Mol Vol | pKa of most Basic/Acidic group | BBB Score |
|---|---|---|---|---|---|---|---|---|---|
| 3,4-Methylenedioxycinnamic acid | C10 H8 O4 | 4 | 1 | 2.34 | 2.65 | 45.74 $A^2$ | 191.44 $A^3$ | <0. / 4.54 | 3.59 |
| Kakuol | C10 H10 O4 | 4 | 1 | 2.40 | 2.39 | 47.15 $A^2$ | 192.64 $A^3$ | <0. / 11.52 | 3.58 |
| Benzyl benzoate | C14 H12 O2 | 2 | 0 | 3.74 | 3.78 | 21.10 $A^2$ | 204.05 $A^3$ | <0. / 24.45 | 5.16 |
| Elemol | C15 H26 O | 1 | 1 | 4.62 | 4.20 | 16.15 $A^2$ | 298.40 $A^3$ | <0. / 15.53 | 4.39 |
| Cubebol | C15 H26 O | 1 | 1 | 3.74 | 3.48 | 16.29 $A^2$ | 283.23 $A^3$ | <0. / 15.70 | 4.39 |
| Moupinamide | C18 H19 N O4 | 4 | 3 | 2.45 | 2.78 | 66.08 $A^2$ | 323.94 $A^3$ | 0.90 / 9.69 | 3.05 |

**Swiss ADME calculation for various pharmacokinetics, water solubility, lipophilicity parameters of chemical constituents of black pepper**

The six compounds exhibit similar solubility and gastrointestinal (GI) absorption but differ in blood-brain barrier (BBB) permeability, CYP1A2 inhibition, lipophilicity, and synthetic accessibility, all of which influence their pharmacological potential. All compounds are water-soluble, aiding absorption and distribution, with high GI absorption enhancing their suitability for oral administration. However, only C-1 to C-5 are BBB permeant, making them candidates for central nervous system (CNS) applications, while C-6 lacks this ability. CYP1A2 inhibition varies, with C-1, C-2, and C-3 acting as inhibitors, potentially causing drug-drug interactions by altering the metabolism of other pharmaceuticals, whereas C-4, C-5, and C-6 do not inhibit CYP1A2, reducing the risk of metabolic interference. Lipophilicity, measured by Log Po/w, affects membrane permeability, with values ranging from 1.80 (C-1) to 3.20 (C-4). Lower lipophilicity (C-1) improves solubility but may limit passive diffusion, while higher lipophilicity (C-4) enhances permeability, including BBB penetration,

but could reduce aqueous solubility. C-2, C-3, C-5, and C-6 fall within a moderate range, balancing solubility and permeability for effective systemic distribution. Synthetic accessibility scores indicate ease of synthesis, with C-3 (1.44) being the easiest to synthesize, making it commercially viable, while C-5 (4.13) is the most complex, requiring intricate production processes (Table 3).

**Table 3.** Swiss ADME data base for various pharmacokinetics, water solubility, lipophilicity and medicinal properties of chemicals selected from black pepper

| **Properties** | **Sub properties** | **C-1** | **C-2** | **C-3** | **C-4** | **C-5** | **C-6** |
|---|---|---|---|---|---|---|---|
| Water solubility | Class | Soluble | Soluble | Soluble | Soluble | Soluble | Soluble |
| Pharmacokinetic | GI absorption | High | high | high | high | high | high |
| | BBB permeant | Yes | yes | yes | yes | Yes | No |
| | CYp1A2 inhibition | Yes | yes | yes | No | No | |
| Lipophilicity | Log $P_{o/w}$ (iLOGP) | 1.80 | 2.27 | 2.68 | 3.20 | 3.10 | 2.58 |
| Medicinal Chemistry | Synthetic accessibility | 2.30 | 2.25 | 1.44 | 3.54 | 4.13 | 2.55 |

The lenlngth of compounds(Table.4)

| Compounds | MAX | VAN | TOB10 | AML10 | COL10 |
|---|---|---|---|---|---|
| Lungs | 2cm | 1.5cm | 4mm | 5mm | 5mm |
| Spleen | 1cm | 2mm | 4mm | 2cm | 4mm |
| Heart | | | | | |

**Pharmacokinetic Parameters (ADMET analysis of compounds)**

The pharmacokinetic analysis of the selected phytochemicals (C-1 to C-6) reveals significant variations in their ADMET properties, affecting their absorption, distribution, metabolism, excretion, and toxicity. All compounds exhibit poor water solubility, with C-4 (-4.666) and C-5 (-4.499) being the least soluble, potentially impacting their formulation and bioavailability. C-3 shows the highest Caco-2 permeability (1.939), indicating superior intestinal absorption, while all compounds exhibit high human intestinal absorption (89.639%–96.169%), suggesting strong oral bioavailability. Skin permeability varies, with C-3 (-1.875) and C-4 (-1.578) demonstrating better transdermal penetration. P-glycoprotein (P-gp) substrate analysis identifies C-3 and C-6 as substrates, potentially affecting their efflux and absorption, though none inhibit P-gp, minimizing drug-drug interaction risks. Distribution parameters indicate that C-5 (0.538) has the highest volume of distribution, favoring tissue penetration, while C-1 (-0.697) remains plasma-retained. C-2 has the highest fraction unbound in plasma (0.426), enhancing free drug availability, whereas C-6 (-0.558) and C-1 (-0.185) show limited blood-brain barrier (BBB) permeability, suggesting minimal central nervous system (CNS) effects. In contrast, C-5 (0.683) and C-4 (0.632) demonstrate higher CNS penetration, making them potential neurological agents. Metabolic analysis suggests all compounds bypass CYP2D6 metabolism risks, but C-3, C-5, and C-6 are CYP3A4 substrates, indicating hepatic metabolism. While C-3 inhibits CYP1A2, CYP2C9, and CYP2C19, raising metabolic interaction concerns, none inhibit CYP3A4, reducing drug-drug interference risks. Excretion profiles show C-4 has the highest clearance (1.311), indicating rapid elimination, whereas C-2 and C-6 clear more slowly (0.231, 0.29), suggesting prolonged systemic presence. Toxicity evaluation confirms no AMES toxicity risks, but C-6 inhibits hERG II, necessitating further cardiac safety assessments. Acute

toxicity (LD50) values indicate C-3 (1.771) and C-4 (1.676) have higher toxicity, while C-1 (2.226) and C-6 (2.036) appear safer. Chronic toxicity (LOAEL) values reveal C-4 (1.164) as the most concerning, while C-1 (2.62) and C-6 (2.425) show lower long-term risks. Only C-1 exhibits hepatotoxicity, warranting liver monitoring in therapeutic applications. Additionally, skin sensitization in C-3, C-4, and C-5 suggests possible allergic reactions. Environmental toxicity tests highlight high *Tetrahymena pyriformis* toxicity in C-3 and C-4, while minnow toxicity is most pronounced in C-1 (1.942) and C-2 (1.636), raising ecological concerns. (table.5)

**Table: pkCSM pharmacokinetic parameters of the selected phytochemicals of**

| **Pharmacokinetic Properties** | | **Selected Phytochemicals** | | | | | |
|---|---|---|---|---|---|---|---|
| **Properties** | **Model Name** | **C-1** | **C-2** | **C-3** | **C-4** | **C-5** | **C-6** |
| Absorption | Water solubility | -1.603 | -2.64 | -3.197 | -4.666 | -4.499 | -3.204 |
| | Caco2 permeability | 1.215 | 1.21 | 1.939 | 1.508 | 1.551 | 0.996 |
| | Intestinal absorption (human) | 93.972 | 94.832 | 96.169 | 93.266 | 93.138 | 89.639 |
| | Skin Permeability | -2.71 | -2.842 | -1.875 | -1.578 | -2.177 | -2.826 |
| | P-glycoprotein substrate | NO | NO | YES | NO | NO | YES |
| | P-glycoprotein I inhibitor | NO | NO | NO | NO | NO | NO |
| | P-glycoprotein II inhibitor | NO | NO | NO | NO | NO | NO |
| Distribution | VDss (human) | -0.697 | 0.151 | 0.171 | 0.406 | 0.538 | 0.245 |
| | Fraction unbound (human) | 0.338 | 0.426 | 0.069 | 0.241 | 0.21 | 0.105 |
| | BBB permeability | -0.185 | 0.401 | 0.268 | 0.632 | 0.683 | -0.558 |
| | CNS permeability | -2.435 | -2.898 | -1.395 | -2.141 | -1.846 | -2.552 |
| Metabolism | CYP2D6 substrate | NO | NO | NO | NO | NO | NO |
| | CYP3A4 substrate | NO | NO | YES | NO | YES | YES |
| | CYP1A2 inhibitor | NO | NO | YES | NO | YES | YES |
| | CYP2C19 inhibitor | NO | NO | YES | NO | NO | NO |
| | CYP2C9 inhibitor | NO | NO | YES | NO | NO | NO |
| | CYP2D6 inhibitor | NO | NO | NO | NO | NO | NO |
| | CYP3A4 inhibitor | NO | NO | NO | NO | NO | NO |
| Excretion | Total Clearance | 0.507 | 0.231 | 0.658 | 1.311 | 0.885 | 0.29 |
| | Renal OCT2 substrate | NO | NO | YES | NO | NO | NO |
| Toxicity | AMES toxicity | NO | NO | NO | NO | NO | NO |
| | Max. tolerated dose (human) | 0.54 | 0.541 | 0.666 | 0.203 | -0.261 | -0.528 |
| | hERG I inhibitor | NO | NO | NO | NO | NO | NO |
| | hERG II inhibitor | NO | NO | NO | NO | NO | YES |
| | Oral Rat Acute Toxicity (LD50) | 2.226 | 1.889 | 1.771 | 1.676 | 1.691 | 2.036 |
| | Oral Rat Chronic Toxicity (LOAEL) | 2.62 | 2.507 | 2.127 | 1.164 | 1.234 | 2.425 |
| | Hepatotoxicity | YES | NO | NO | NO | NO | NO |
| | Skin Sensitization | NO | NO | YES | YES | YES | NO |
| | *T.Pyriformis* toxicity | 0.488 | 0.226 | 1.663 | 1.919 | 1.523 | 0.843 |
| | Minnow toxicity | 1.942 | 1.636 | 0.28 | 0.572 | 0.727 | 1.263 |

**(Table.5)**

**Stop tox Toxicity parameters (ADME analysis of compounds)**

Among the six examined compounds, C-5 emerges as the safest, exhibiting non-toxic properties across all tested categories. It has an 89.0% non-toxicity rate for eye exposure, making it the least likely to cause irritation or damage, while maintaining a

broad safety profile in oral (73.0%), cutaneous (60.0%), and inhalation (73.0%) exposure. Additionally, its classification as a non-irritant (60.0%) and non-sensitizer (50.0%) reinforces its suitability for applications involving direct skin contact or unintentional exposure. C-6 closely follows C-5 in safety, with high non-toxicity rates for inhalation (73.0%), dermal (81.0%), and ocular (63.1%) exposure. However, its 50.0% likelihood of causing skin sensitization suggests a potential risk for allergic reactions in sensitive individuals, though it remains generally safe for various applications. C-2 and C-4 exhibit moderate safety profiles, with some toxic risks. C-2 shows toxicity in dermal exposure (64.0%) but remains non-toxic when inhaled (80.0%), ingested (64.0%), or applied topically (61.0%). It is a viable option if skin exposure is minimized. C-4, on the other hand, is toxic in skin irritation (60.0%) and eye irritation (58.0%) but remains non-toxic in inhalation (64.0%), oral (91.0%), and topical (83.0%) exposure, making it suitable for controlled applications that avoid direct contact with sensitive tissues. In contrast, C-1 and C-3 pose the highest toxicity concerns. C-1 exhibits oral toxicity (55.0%) and skin sensitization (70.0%), making it unsuitable for consumer products involving ingestion or prolonged skin contact. C-3 presents the most significant risks, with high oral toxicity (69.0%) and extreme sensitization potential (90.0%), indicating severe adverse effects upon ingestion or repeated skin exposure, despite its non-toxicity in inhalation (61.0%), topical (85.0%), and ocular (85.0%) exposure. Thus, while C-5 and C-6 are the safest options, C-3 and C-1 require caution due to their high toxicity risks. (Table.6)

**Table: StopTox toxicity parameters of the selected phytochemicals of (Table.6)**

| **Ligands** | **Acute Inhalation Toxicity** | **Acute Oral Toxicity** | **Acute Dermal Toxicity** | **Eye Irritation and Corrosion** | **Skin Sensitization** | **Skin Irritation and Corrosion** |
|---|---|---|---|---|---|---|
| | | | | | | |
| C-1 | **Non Toxic (-) 72.0%** | **Toxic (+) 55.0%** | **Non Toxic (-) 53.o%** | **Non Toxic(-) 50.0%** | **Sensitizer (+) 70%** | **Negative (-) 70%** |
| C-2 | **Non Toxic (-) 80.0%** | **Non Toxic(-) 64.0%** | **Toxic (+) 64.0%** | **Non Toxic (-) 61.0%** | **Non-Sensitizer (-) 60%** | **Negative (-)** 70 |
| C-3 | **Non Toxic (-) 61.0%** | **Toxic(+) 69.0%** | **Non Toxic(-) 85.0%** | **Non Toxic (-) 85.0%** | **Sensitizer (+) 90%** | **Negative (-)** 90% |
| C-4 | **Non Toxic (-) 64.0%** | **Non Toxic (-) 91.0%** | **Non Toxic (-) 83.0%** | **Toxic(+) 58.0 %** | **Non-Sensitizer (-)** 50% | **Positive (+) 60%** |
| C-5 | **Non Toxic (-) 60.0%** | **Non Toxic (-) 69.0%** | **Non Toxic (-) 73.0%** | **Non Toxic (-) 89.0%** | **Non-Sensitizer (-) 50%** | **Negative (-)** 60% |
| C-6 | **Non Toxic (-) 73.0%** | **Non Toxic (-) 67.0%** | **Non Toxic (-) 81.0%** | **Non Toxic (-) 63.0%** | **Sensitizer (+) 50%** | **Negative (-)** 80% |

**Pass calculation parameters (ADME analysis of compounds**

The inhibition of bacterial efflux pumps has emerged as a key strategy in overcoming antibiotic resistance, with C-6 (Pa = 0.212, Pi = 0.002) and C-5 (Pa = 0.200, Pi = 0.040) showing the most promise in this area. These findings, based on the PASS

(Prediction of Activity Spectra for Substances) model, indicate that different compounds exhibit varying antibacterial, enzyme-inhibitory, and immune-modulating activities. Higher Pa values suggest a greater likelihood of activity, while higher Pi values indicate reduced effectiveness. C-4 (Pa = 0.434, Pi = 0.031) and C-3 (Pa = 0.376, Pi = 0.046) are the best candidates for anti-mycobacterial activity, making them potential treatments for tuberculosis. C-4 and C-5 also display the strongest general antibacterial properties, while C-6 exhibits weak antibacterial activity (Pa = 0.184, Pi = 0.133). Enzyme inhibition analysis highlights that C-4 (Pa = 0.190) and C-2 (Pa = 0.179) have the highest phospholipase A2 inhibition, suggesting anti-inflammatory potential, whereas C-6 is the least effective in this regard. Peptidoglycan glycosyltransferase inhibition, critical for bacterial cell wall synthesis, is strongest in C-5 (Pa = 0.577) and C-3 (Pa = 0.510), while C-4 shows the lowest activity. Additionally, C-2 and C-6 inhibit topoisomerase I, suggesting antibacterial and anticancer potential. RNA-directed RNA polymerase inhibition, relevant for antiviral and antibacterial activity, is most notable in C-3 and C-1. Furthermore, C-6 exhibits the highest potential in mimicking antimicrobial peptides like lactoferrin, defensin, and cathelicidin, highlighting its immune-boosting properties, with C-5 and C-4 also demonstrating strong immune-regulating effects.

**Table: PASS calculations of main compounds in the tested extracts for their observed biological activities. (Table.7)**

Pa: probable activity; Pi: probable inactivity

| **Biological assays** | **Pass prediction** | | | | | | | | | | | |
|---|---|---|---|---|---|---|---|---|---|---|---|---|
| | **C-1** | | **C-2** | | **C-3** | | **C-4** | | **C-5** | | **C-6** | |
| | **Pa** | **Pi** | **Pa** | **Pi** | **Pa** | **Pi** | **Pa** | **Pi** | **Pa** | **pi** | **pa** | **pi** |
| Antimycobacterial | 0,287 | 0,089 | 0,251 | 0,118 | 0,376 | 0,046 | 0,434 | 0,031 | 0.300 | 0.080 | 0,250 | 0,119 |
| Antibacteria | 0,263 | 0,076 | 0,264 | 0,075 | 0,262 | 0,077 | 0,474 | 0,019 | 0,401 | 0,030 | 0,184 | 0,133 |
| Bacterial efflux pump inhibitor | 0,118 | 0,11 | 0,067 | 0,036 | 0,144 | 0,024 | 0.120 | 0.080 | 0.200 | 0.040 | 0,212 | 0,002 |
| Lysozyme inhibitor | 0,102 | 0,067 | 0,098 | 0,071 | 0,178 | 0,029 | 0.150 | 0.060 | 0.140 | 0.070 | 0.130 | 0.065 |
| Phospholipase A2 inhibitor | 0,155 | 0,042 | 0,179 | 0,032 | 0,176 | 0,033 | 0.190 | 0.040 | 0.160 | 0.050 | 0,112 | 0,074 |
| Peptidoglycan glycosyltransferase inhibitor | 0,474 | 0,028 | 0,402 | 0,051 | 0,510 | 0,020 | 0,367 | 0,067 | 0,577 | 0,010 | 0.410 | 0.045 |
| RNA-directed RNA polymerase inhibitor | 0,404 | 0,050 | 0,382 | 0,067 | 0,434 | 0,031 | 0.390 | 0.070 | 0,340 | 0,106 | 0.360 | 0.090 |
| Lactoferrin | 0.587 | 0.413 | 0.823 | 0.177 | 0.528 | 0.472 | 0.691 | 0.309 | 0.793 | 0.207 | 0.901 | 0.099 |
| Defensin | 0.671 | 0.329 | 0.742 | 0.258 | 0.581 | 0.419 | 0.761 | 0.239 | 0.849 | 0.151 | 0.956 | 0.044 |
| Cathelicidin | 0.6 | 0.3 | 0.7 | 0.2 | 0.5 | 0.4 | 0.7 | 0.2 | 0.8 | 0.17 | 0.9 | 0.0 |

| | 01 | 99 | 85 | 15 | 55 | 45 | 29 | 71 | 23 | 7 | 27 | 73 |
|---|---|---|---|---|---|---|---|---|---|---|---|---|
| Azurocidin | 0.655 | 0.345 | 0.758 | 0.242 | 0.569 | 0.431 | 0.748 | 0.252 | 0.835 | 0.165 | 0.943 | 0.057 |
| Bpi | 0.632 | 0.368 | 0.812 | 0.188 | 0.549 | 0.451 | 0712 | 0.288 | 0.805 | 0.195 | 0.914 | 0.086 |
| Magainin | 0.693 | 0.307 | 0.699 | 0.301 | 0.604 | 0.396 | 0.784 | 0.216 | 0.863 | 0.137 | 0.967 | 0.033 |
| Cecropin | 0.624 | 0.376 | 0.729 | 0.271 | 0.561 | 0.439 | 0.738 | 0.262 | 0.828 | 0.172 | 0.935 | 0.065 |
| Protegrin | 0.661 | 0.339 | 0754 | 0.246 | 0.585 | 0.415 | 0.756 | 0.244 | 0.843 | 0.157 | 0.951 | 0.049 |
| Histatin | 0.598 | 0.402 | 0.682 | 0.318 | 0.535 | 0.465 | 0.698 | 0.302 | 0.794 | 0.206 | 0.904 | 0.096 |
| Lactoferricin | 0.617 | 0.363 | 0771 | 0.229 | 0.554 | 0.446 | 0.725 | 0.275 | 0.819 | 0.181 | 0.923 | 0.077 |
| Granulysin | 0.649 | 0.351 | 0.748 | 0.252 | 0.573 | 0.427 | 0.744 | 0.256 | 0.831 | 0.169 | 0.941 | 0.059 |
| Dermcidin | 0.636 | 0.364 | 0.736 | 0.264 | 0.558 | 0.442 | 0.732 | 0.268 | 0.824 | 0.176 | 0.929 | 0.071 |
| LL-37 | 0.674 | 0.326 | 0.725 | 0.275 | 0.595 | 0.403 | 0.769 | 0.231 | 0.854 | 0.146 | 0.958 | 0.042 |
| Psoriasin | 0.609 | 0.391 | 0.759 | 0.241 | 0.548 | 0.452 | 0.714 | 0.286 | 0.808 | 0.192 | 0.918 | 0.082 |
| Calprotectin | 0.594 | 0.406 | 0.805 | 0.195 | 0.529 | 0.471 | 0.689 | 0.311 | 0.796 | 0.204 | 0.906 | 0.094 |

**Pro-Tox 11mtoxicological parameters (ADME analysis of compounds)**

The toxicity analysis of compounds C-1 to C-6 evaluates potential harmful effects across various endpoints, including organ toxicity, carcinogenicity, immunotoxicity, mutagenicity, cytotoxicity, nuclear receptor signaling, and stress response pathways. The categorization (Pre) identifies whether a compound is active (A) or inactive (I), while probability (Pro) values indicate the likelihood of toxicity. All six compounds are considered inactive for hepatotoxicity, meaning they are unlikely to cause liver damage, with C-5 and C-6 showing the highest probability (0.77) and C-3 the lowest (0.67). Carcinogenicity predictions classify C-1, C-2, and C-3 as active, with C-1 showing the highest likelihood (0.76), while C-4, C-5, and C-6 are inactive, suggesting a lower risk. Immunotoxicity results indicate C-1, C-2, and C-6 as active, with C-1 (0.85) and C-6 (0.94) having the highest probability of immune system effects. For mutagenicity, C-3 is active (0.54), while other compounds are inactive but with varying probabilities, with C-4 (0.85) and C-5 (0.75) showing the lowest mutagenic risk. Cytotoxicity predictions classify all compounds as inactive, with C-3 (0.91) and C-6 (0.98) having the highest likelihood of cellular damage. In nuclear receptor signaling, C-3 and C-4 exhibit the highest probabilities (0.99) for AhR and AR interactions, indicating potential biological effects. Stress response pathway predictions classify all compounds as inactive, but C-3 shows the highest probability for p53 (0.99) and HSE (1.0), suggesting an influence on cellular stress responses, while C-4 has the highest probability (0.99) in the DNA damage ATAD5 pathway (Table.8).

**Table: Pro-Tox II toxicological parameters of the identified phytoconstituents of(Table.8)**

| Classification | Target | C-1 | | C-2 | | C-3 | | C-4 | | C-5 | | C-6 | |
|---|---|---|---|---|---|---|---|---|---|---|---|---|---|
| | | Pre | Pro | Pre | Pro | Pre | Pro | Pre | Pro | Pre | Pro | Pre | Pro |
| Organ toxicity | Hepatotoxicity | I | 0.73 | 1 | 0.72 | I | 0.67 | I | 0.74 | I | 0.77 | I | 0.77 |
| Toxicity end points | Carcinogenicity | A | 0.76 | A | 0.55 | A | 0.55 | I | 0.77 | I | 0.75 | I | 0.57 |
| | Immunotoxicity | A | 0.85 | A | 0.51 | I | 0.99 | I | 0.99 | I | 0.85 | A | 0.94 |
| | Mutagenicity | I | 0.71 | I | 0.63 | A | 0.54 | I | 0.85 | I | 0.75 | I | 0.61 |
| | Cytotoxicity | I | 0.88 | I | 0.88 | I | 0.91 | I | 0.73 | I | 0.86 | I | 0.98 |
| Tox21-Nuclear receptor signalling pathways | AhR | I | 0.51 | I | 0.76 | I | 0.99 | I | 0.99 | I | 0.99 | I | 0.89 |
| | AR | I | 0.82 | I | 0.80 | I | 1.0 | I | 0.99 | I | 0.65 | I | 0.99 |
| | AR-LBD | I | 0.83 | I | 0.84 | I | 1.0 | I | 0.99 | I | 0.87 | I | 0.99 |
| | Aromatase | I | 0.99 | I | 0.98 | I | 0.99 | I | 0.92 | I | 0.99 | I | 0.87 |
| | ER | I | 0.96 | I | 0.94 | I | 0.71 | I | 0.95 | I | 0.60 | I | 0.90 |
| | ER-LBD | I | 0.98 | I | 0.97 | I | 0.99 | I | 0.93 | I | 0.61 | I | 0.98 |
| | PPAR-Gamma | I | 0.96 | I | 0.95 | I | 0.98 | I | 0.94 | I | 0.99 | I | 0.91 |
| | nrf2/ARE | I | 0.93 | I | 0.94 | I | 1.0 | I | 0.87 | I | 0.90 | I | 0.93 |
| Tox21-Stress response pathways | HSE | I | 0.93 | I | 0.94 | I | 1.0 | I | 0.87 | I | 0.90 | I | 0.93 |
| | MMP | I | 0.96 | I | 0.81 | I | 0.98 | I | 0.80 | I | 0.53 | I | 0.80 |
| | p53 | I | 0.97 | I | 0.83 | I | 0.99 | I | 0.99 | I | 0.97 | I | 0.90 |
| | ATAD5 | I | 0.97 | I | 0.95 | I | 0.91 | I | 0.99 | I | 0.98 | I | 0.89 |

**Radar Plot Analysis of Molecular Properties**

The radar plots (A–F) illustrate the variation in molecular properties across different compounds, considering six key parameters: lipophilicity (LIPO), size, polarity (POLAR), insolubility (INSOLU), unsaturation (INSATU), and flexibility (FLEX). Each plot shows a distinct molecular profile, with some compounds displaying higher lipophilicity (A, C, F), while others exhibit greater polarity or insolubility (B, D, E). The differences in these properties suggest variations in solubility, membrane permeability, and potential biological activity, which are crucial for drug design and optimization. These findings provide insight into the molecular characteristics that may influence pharmacokinetic and pharmacodynamic behavior (Figure 1).

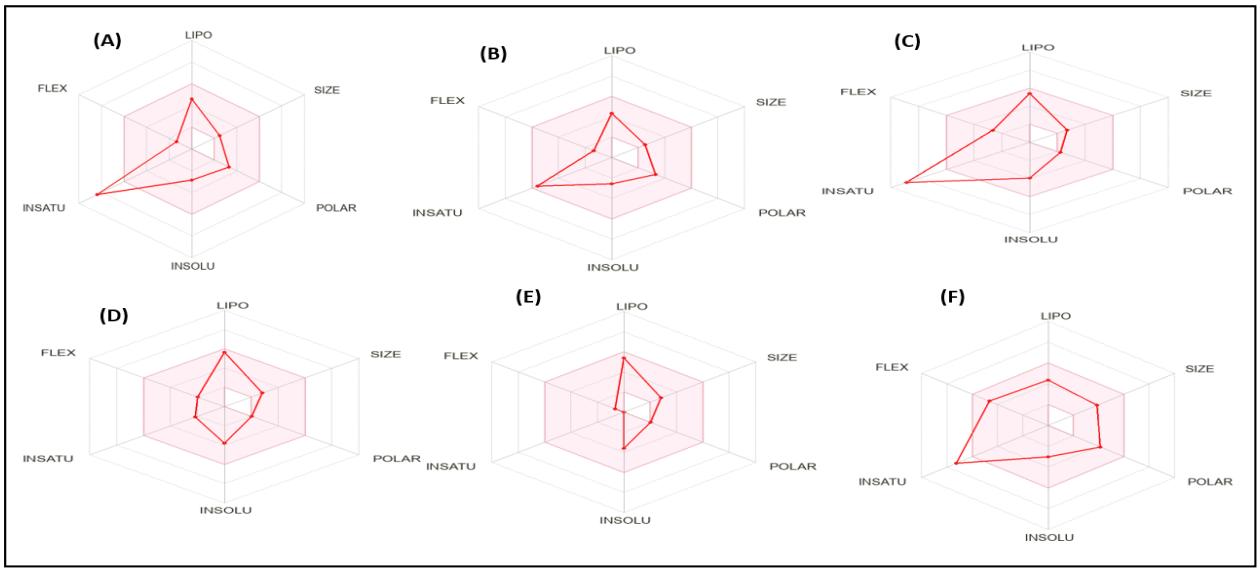


Figure 1: The radar plots (A–F) depict the molecular property distributions of different compounds based on six parameters: lipophilicity (LIPO), size, polarity

(POLAR), insolubility (INSOLU), unsaturation (INSATU), and flexibility (FLEX). The red lines represent the property profiles of each compound, while the shaded regions indicate the comparative distribution range. Variations in each plot suggest differences in molecular characteristics, with some compounds exhibiting higher lipophilicity (A, C, F), while others show increased polarity or insolubility (B, D, E). The results highlight diverse physicochemical properties, which could influence biological activity and pharmacokinetics.

**Probability Distribution of Molecular Activity**

The radar plots illustrate the predicted probability distributions of molecular activity, comparing individual molecules (gray regions) against the average profile of known active molecules (orange regions). The extent of overlap indicates how closely each molecule aligns with established bioactive compounds. Some molecules (e.g., A, B, F) exhibit lower probabilities across multiple targets, suggesting limited predicted activity, whereas others (e.g., C, D, E) display greater overlap, implying stronger potential as bioactive compounds. These variations highlight key differences in molecular interactions, which can guide drug discovery efforts by prioritizing compounds with higher predicted activity for further validation (Figure 2).

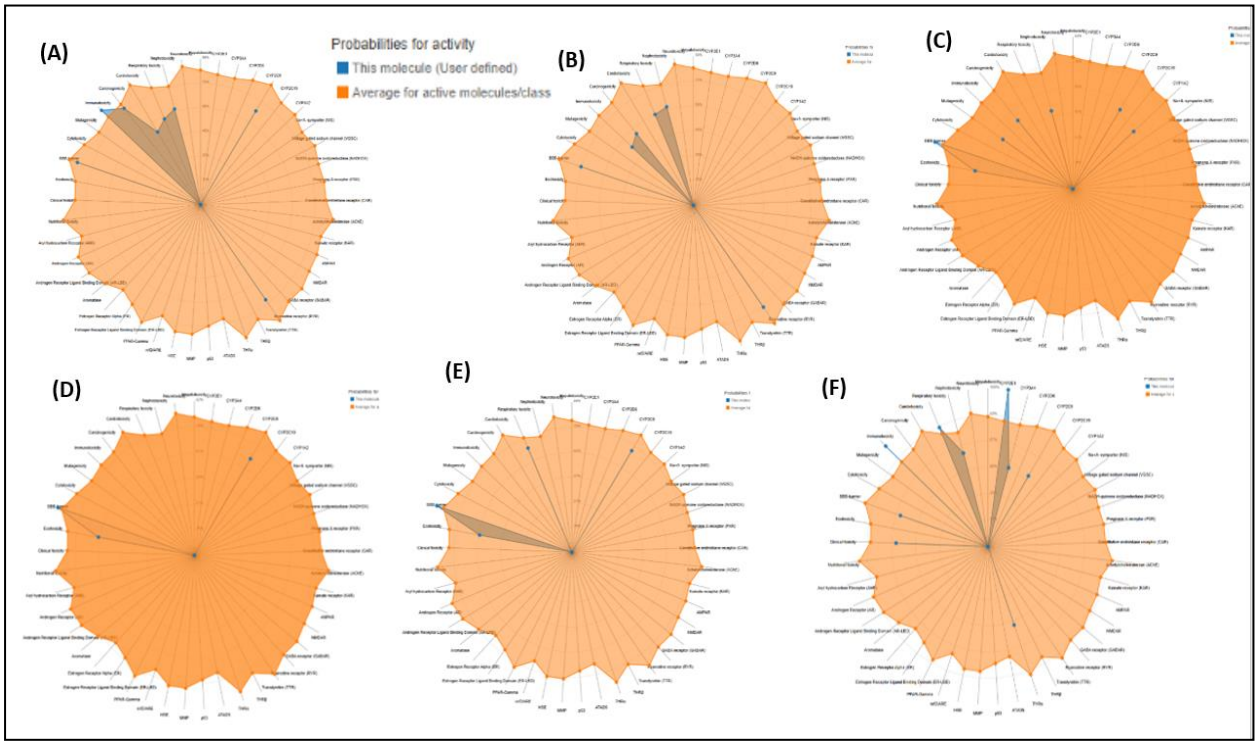


Figure 2: The radar plots (A–F) depict the predicted probabilities for biological activity across various molecular targets. The orange regions represent the average probability distribution for active molecules in the given class, while the overlaid gray areas highlight the specific probability values for the analyzed molecules. Variations in overlap suggest differing degrees of alignment with known active molecules, with some compounds (e.g., A, B, F) exhibiting lower probabilities for multiple targets, while others (e.g., C, D, E) show closer alignment with active molecular profiles. These insights can aid in identifying potential drug candidates by assessing their predicted activity across multiple targets.

**Target Interaction Network of Molecular Clusters**

The target interaction networks demonstrate the predicted binding affinity of molecular clusters to various biological targets, with the inactive cluster (blue) serving as a central hub. Green nodes represent specific proteins, including metabolic

enzymes (e.g., CYP3A4, CYP2C9) and receptor targets (e.g., GABA, NMDA). The connectivity pattern reveals potential pharmacological and metabolic interactions, with CYP3A4 frequently appearing as a key target, indicating its importance in drug metabolism. Differences in interaction patterns suggest variations in bioactivity, guiding the selection of molecules with desirable target profiles for further experimental validation (Figure 3).

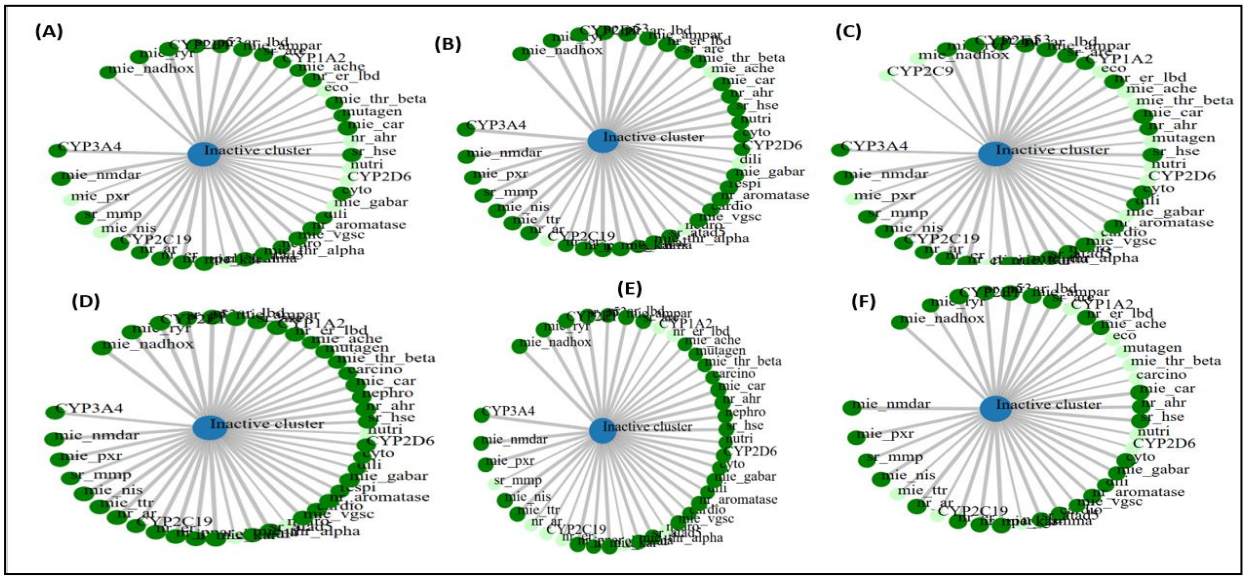


Figure 3: The network diagrams (A–F) illustrate the predicted interactions of different molecular clusters with various biological targets. The blue node represents the inactive cluster, while the green nodes correspond to potential molecular targets, including enzymes, receptors, and transporters. Lines connecting the inactive cluster to target nodes indicate predicted interactions. Across all panels, CYP3A4 appears as a recurring target, suggesting its significant role in drug metabolism. Variations in network density and target distribution reflect differences in molecular activity profiles, which can inform drug design and optimization strategies.

**Predicted Toxicity and Metabolic Risk Network**

The network diagrams illustrate the predicted toxicological and metabolic risks associated with different molecular clusters. The active clusters (blue nodes) are linked to various toxicity-related endpoints (red nodes), including organ toxicity (nephro, cardio), metabolic interactions (CYP2C9, CYP3A4), and potential mutagenicity. Some molecular clusters (e.g., B, C, F) exhibit multiple risk connections, suggesting a higher likelihood of adverse effects, while others (e.g., D, E) display fewer associations, indicating potentially safer profiles. The presence of CYP enzyme interactions suggests potential drug metabolism issues, which could impact pharmacokinetics. These insights aid in assessing the drug-likeness and safety of the analyzed compounds, informing further optimization and selection (Figure 4).

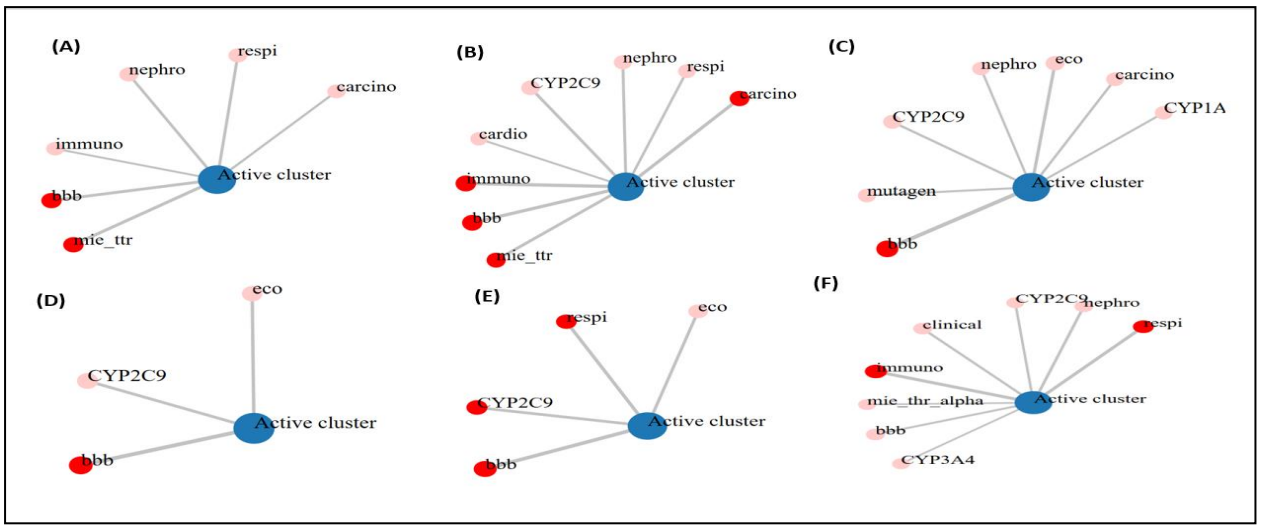


Figure 4: The network diagrams (A–F) represent the predicted associations between active molecular clusters (blue nodes) and various toxicity or metabolic risk factors (red nodes). Each red node corresponds to a specific risk category, including nephrotoxicity (nephro), cardiotoxicity (cardio), immunotoxicity (immuno), blood-brain barrier penetration (bbb), respiratory toxicity (respi), carcinogenicity (carcino), and interactions with metabolic enzymes (e.g., CYP2C9, CYP1A, CYP3A4). The strength and number of connections indicate the extent to which each molecular cluster is linked to these risks. Differences across the networks highlight the varying safety profiles of different molecular clusters, which can help guide the selection of safer drug candidates.

**Zone of inhibition of E. coli by BPP Extracts**

The agar well diffusion assay results indicate that both BPP methanol and water extracts exhibit notable antimicrobial activity, as shown by the clear inhibition zones around the wells. The TE (30 mg) extract demonstrated a smaller inhibition zone, suggesting lower antimicrobial efficacy. The bar graphs quantitatively confirm these findings, with statistically significant differences in inhibition zones, where BPP methanol and water extracts consistently show greater antibacterial effects compared to TE. These results highlight the potential of plant extracts as natural antimicrobial agents, with methanol and water extracts demonstrating superior activity (Figure 5).

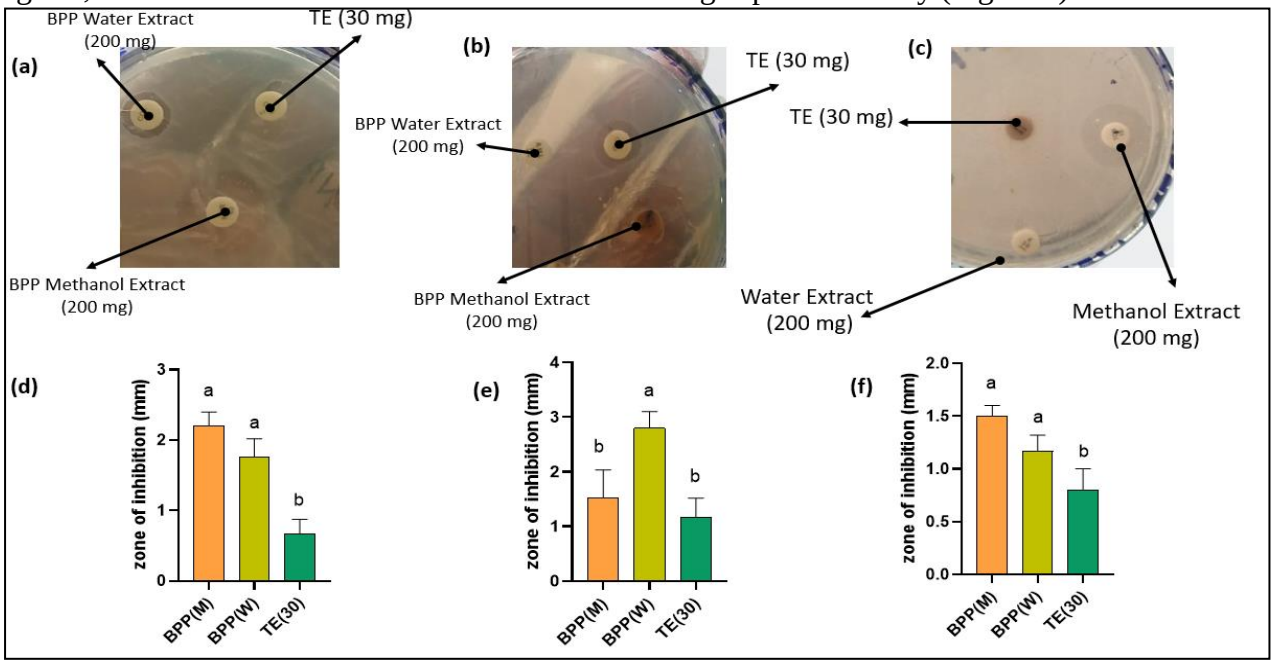

Figure 5: The images (a–c) show agar well diffusion assays used to assess the antimicrobial activity of different plant extracts, including BPP water extract (200 mg), BPP methanol extract (200 mg), and TE (30 mg). The clear zones around the wells indicate inhibition of bacterial growth. The bar graphs (d–f) represent the zone of inhibition (mm) for each extract, with statistical significance indicated by different letters (a, b). Larger inhibition zones suggest stronger antimicrobial activity, with BPP methanol and water extracts exhibiting higher activity than TE. These findings suggest that plant extracts, particularly methanol and water extracts, possess significant antimicrobial potential.

**Zone of inhibition of Salmonella by BPP Extracts**

The agar diffusion assay results demonstrate that both BPP methanol and water extracts possess considerable antimicrobial activity, as evidenced by the larger inhibition zones around the wells. TE (30 mg) showed a smaller inhibition zone, indicating lower antimicrobial efficacy. The bar graphs confirm these findings, showing statistically significant differences among the extracts, with BPP methanol and water extracts having the highest antibacterial potential. These results highlight the effectiveness of plant-derived extracts as antimicrobial agents, with methanol and water extracts displaying superior inhibitory activity(Figure6).

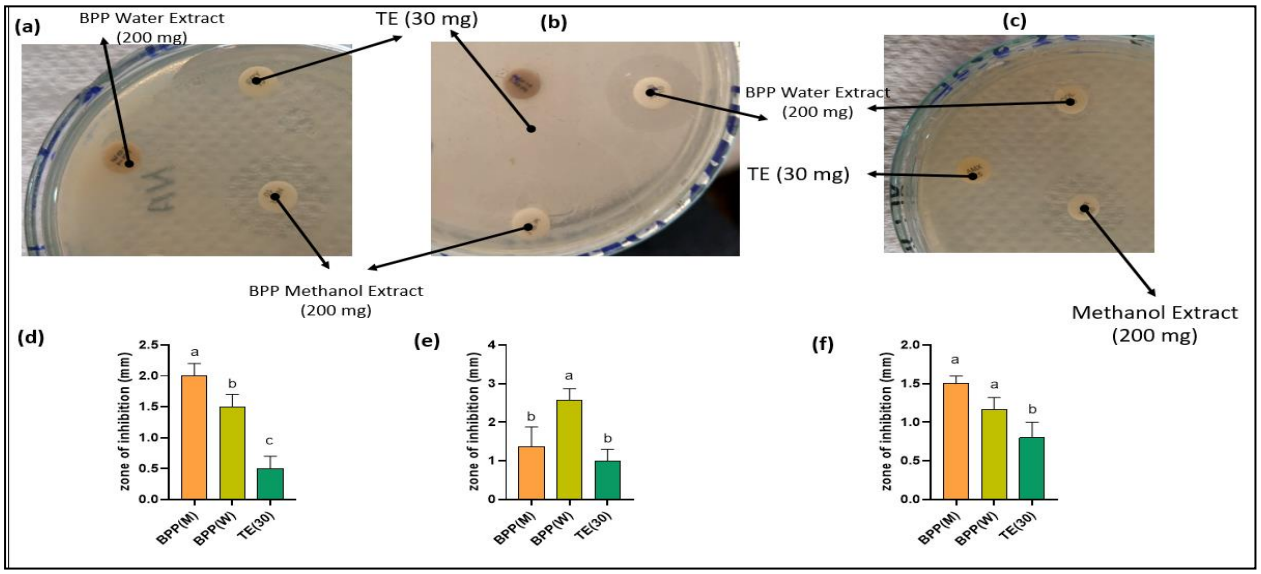


Figure 6: The images (a–c) display agar well diffusion assays evaluating the antimicrobial efficacy of different plant extracts, including BPP water extract (200 mg), BPP methanol extract (200 mg), and TE (30 mg). Clear zones around the wells indicate bacterial growth inhibition. The bar graphs (d–f) quantify the zone of inhibition (mm) for each extract, with statistical significance represented by different letters (a, b, c). The results indicate that the BPP methanol and water extracts exhibit significantly larger inhibition zones compared to TE, suggesting their stronger antimicrobial activity.

**Microscopic Analysis of Bacterial Biofilm Formation by gram staining**

The microscopic analysis reveals a significant difference in biofilm formation between the two samples. In image (a), fewer bacterial clusters are observed, indicating weak biofilm formation, possibly due to unfavorable conditions or antimicrobial treatment. In contrast, image (b) exhibits dense bacterial aggregation and extracellular matrix deposition, signifying robust biofilm formation. This suggests that certain conditions or factors promote bacterial adherence and biofilm development, which could have implications for infection control and antimicrobial strategies (Figure 7).

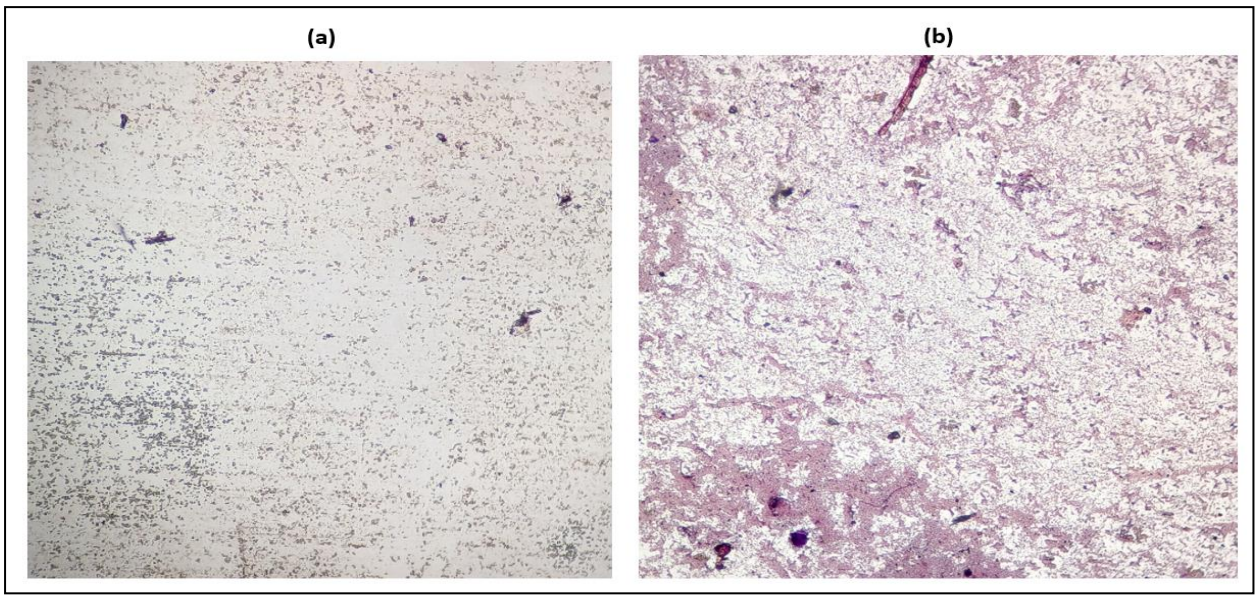


Figure 7: The microscopic images (a) and (b) show bacterial biofilm formation under different conditions. Image (a) represents a control sample with minimal biofilm formation, while image (b) shows extensive biofilm formation, indicating a dense bacterial matrix. The increased biofilm density in (b) suggests enhanced bacterial aggregation and extracellular matrix production, which could be influenced by environmental factors or treatments. The comparison highlights differences in bacterial adhesion and biofilm development, which are critical for understanding antimicrobial resistance and biofilm-associated infections.

**Biochemical Tests conformation for Bacteria**

The biochemical test results indicate different metabolic capabilities of the bacterial strains tested. In (a), the presence of a brown precipitate suggests the production of hydrogen sulfide ($H_2S$), which is characteristic of certain enteric bacteria. In (B), the blue coloration of the citrate test signifies the bacterium's ability to use citrate as its sole carbon source, a feature of some Gram-negative bacteria such as *Salmonella*. In (c), the darkened slant in the urease test indicates a positive reaction, suggesting the presence of urease enzyme-producing bacteria like *Proteus* or *Helicobacter*. These biochemical assays help in distinguishing bacterial species based on their enzymatic activities and metabolic pathways (Figure 8).

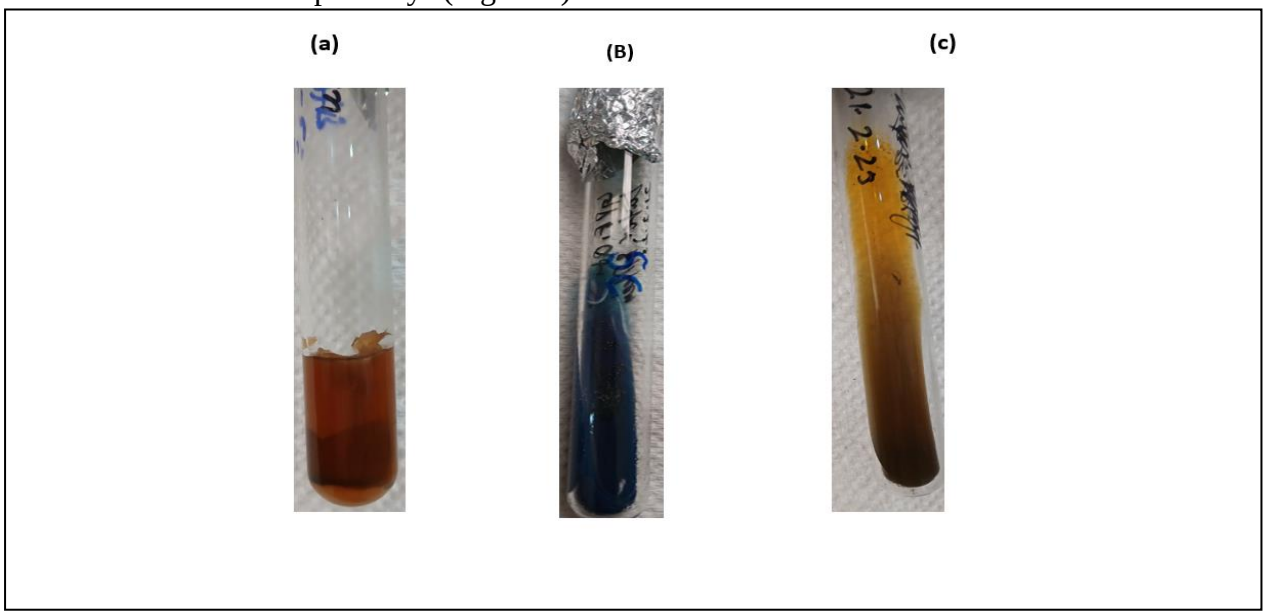


n

Discussion

The study identified six active compounds from black pepper—3,4-Methylenedioxycinnamic Acid, Benzyl Benzoate, Kakuol, Elemol, Cubebol, and Moupinamide—based on their molecular weight, bioavailability, and drug-likeness. Among them, 3,4-Methylenedioxycinnamic Acid had the highest bioavailability (0.85) and the lowest molecular weight (192.17 g/mol), enhancing its absorption potential. Lipophilicity and water solubility varied, with Elemol being the most lipophilic (MolLogP 4.62) and 3,4-Methylenedioxycinnamic Acid the least (MolLogP 2.34). Moupinamide, the most hydrophilic due to high hydrogen bonding potential, had the largest molecular weight (313.35 g/mol), affecting its permeability. Benzyl Benzoate exhibited the highest blood-brain barrier (BBB) penetration potential (5.16), followed by Elemol and Cubebol (4.39), while Moupinamide had the lowest (3.05) due to its large molecular size and hydrogen bonding characteristics. These findings highlight significant differences in physicochemical and pharmacokinetic properties that influence drug-likeness, solubility, permeability, and BBB penetration, crucial for therapeutic applications.

**Active compounds**

Black pepper contains several active compound including 3,4-Methylenedioxycinnamic Acid, Benzyl benzoate, Kakuol, Elemol, Cubebol, & Moupinamide. (POP et al., 2024) reported Black pepper contains bioactive compounds such as piperine, β-caryophyllene, sabinene, and limonene. Similarly another study reported that The bioactive compounds in black pepper include piperine, which exhibits hypolipidemic, antibacterial, neuroprotective, anticancer, anticonvulsant, analgesic, and anti-inflammatory properties (Anandh & Priya, 2024).

**Conclusion**

The study concludes that black pepper (*Piper nigrum*) serves as a potent natural source of antimicrobial agents capable of combating multidrug-resistant pathogens such as *S. aureus* and *E. coli*. By integrating *in vitro* assays with *in silico* molecular docking and ADMET analysis, the research successfully identified key bioactive compounds most notably Cubebol (C-5) that demonstrate high binding affinity to bacterial proteins and favorable safety profiles. These findings suggest that the phytochemicals in black pepper not only inhibit bacterial growth but also hold potential as efflux pump inhibitors to overcome antibiotic resistance. Ultimately, while black pepper shows great promise as a safe and effective therapeutic alternative to conventional antibiotics, further clinical research is recommended to optimize these compounds for pharmaceutical applications in the global fight against antimicrobial resistance.

**References**

Aqeel, A., Amin, A., Sultan, Q. A., Yousaf, I., & Fatima, K. MICROBIAL CONTAMINATION OF STREET FOOD VENDORS'HANDS: PREVALENCE OF STAPHYLOCOCCUS AUREUS AND OTHER PATHOGENS.

Aqeel, A., Jabeen, S., Kainat, T., Ahmed, M., Azhar, I. A., Arain, H., & Khanam, Y. (2025). ROLE OF MICROBIAL CONTAMINANTS IN THE DEVELOPMENT OF MALNUTRITION IN PEDIATRIC PATIENTS WITH GASTROINTESTINAL DISEASES. Frontier in Medical and Health Research, 3(8), 1215-1225.

Aydemir, E., Sarıyer, E., Akyıldız, E., Özad Düzgün, A., Camadan, Y., & Saral Sarıyer, A. (2022). In vitro and in silico evaluation of some plant extracts and phytocompounds against multidrug-resistant Gram-negative bacteria. *Advances in Traditional Medicine*, *22*(4), 749-759.

Dongre, P., Bhambar, R., & Polshettiwar, S. (2022). In silico and Molecular Docking Studies of Black Pepper Phyto-constituents against EmrD Efflux Pump of E. coli. *Indian Journal of Pharmaceutical Education & Research*, *56*(1).

Fratianni, F., Amato, G., Coppola, F., Ombra, M. N., d'Acierno, A., De Martino, L., ... & Nazzaro, F. (2026). In Vitro Evaluation of the Bioactive Potential of Commercial Pepper Essential Oils. *Molecules*, *31*(5), 832.

Iskandar, K., Ahmed, N., Paudyal, N., Ruiz Alvarez, M. J., Balasubramani, S. P., Saadeh, D., ... & Van Dongen, M. (2025). Essential Oils as antimicrobial agents against WHO Priority bacterial pathogens: A strategic review of in vitro clinical efficacy, innovations and research gaps. *Antibiotics*, *14*(12), 1250.

Kiranmayee, M., Rajesh, N., Vidya Vani, M., Khadri, H., Mohammed, A., Chinni, S. V., ... & Moussa, A. Y. (2023). Green synthesis of Piper nigrum copper-based nanoparticles: in silico study and ADMET analysis to assess their antioxidant, antibacterial, and cytotoxic effects. *Frontiers in Chemistry*, *11*, 1218588.

LONGE, B. T. (2025). *ANTIMICROBIAL ACTIVITIES OF SOME SPICE BLENDS ON MULTI-DRUG-RESISTANT BACTERIA ASSOCIATED WITH GASTROINTESTINAL TRACT INFECTIONS* (Doctoral dissertation, FEDERAL UNIVERSITY OF TECHNOLOGY, AKURE).

Periferakis, A. T., Adalis, G. M., Periferakis, A., Troumpata, L., Periferakis, K., Dragosloveanu, C. D. M., ... & Caruntu, C. (2025). The Multifaceted Antimicrobial Profile of Piperine in Infectious Disease Management: Current Perspectives and Potential. *Pharmaceuticals*, *18*(10), 1581.

Rajia, S., Khatun, F., Khanam, A., Anika, M., Rahaman, M. A., Khatun, M. H., & Hasan, I. (2025). Synergistic effect of Piper chaba root extracts and synthesized silver nanoparticles with antibiotics against multidrug-resistant uropathogenic bacteria. *Food Chemistry Advances*, *9*, 101155.

Singh, K., Jain, D., Chaitanya, M. V. N. L., & Kumar, S. (2024). A review of molecular investigations on traditional Chinese medicinal plant-based therapies in multidrug-resistant tuberculosis. *Pharmacological Research*, *13*(10052), 1.

Yasir, B., Mus, S., Rahimah, S., Tandiongan, R. M., Klara, K. P., Afrida, N., ... & Rohman, A. (2024). Antimicrobial Profiling of Piper betle L. and Piper nigrum L. Against Methicillin-Resistant Staphylococcus aureus (MRSA): Integrative Analysis of Bioactive Compounds Based on FT-IR, GC-MS, and Molecular Docking Studies. *Separations*, *11*(11), 322.